Electronic Supplementary Material (ESI) for Inorganic Chemistry Frontiers.

Supporting Information

for the publication "Isoreticular design of flexible Zn-based tetracarboxylate MOFs"

Bodo Felsner*[a], Volodymyr Bon[a], Christopher Bachetzky[b], Eike Brunner[b], Stefan Kaskel[a]

a. Department for Inorganic Chemistry I, Technical University Dresden, Bergstraße 66, 01069 Dresden, Germany

b. Department for Bioanalytical Chemistry, Technical University Dresden, Bergstraße 66, 01069 Dresden, Germany

1. IR and NMR Spectra for Linker Characterization

1.1. Et_4tpdatb

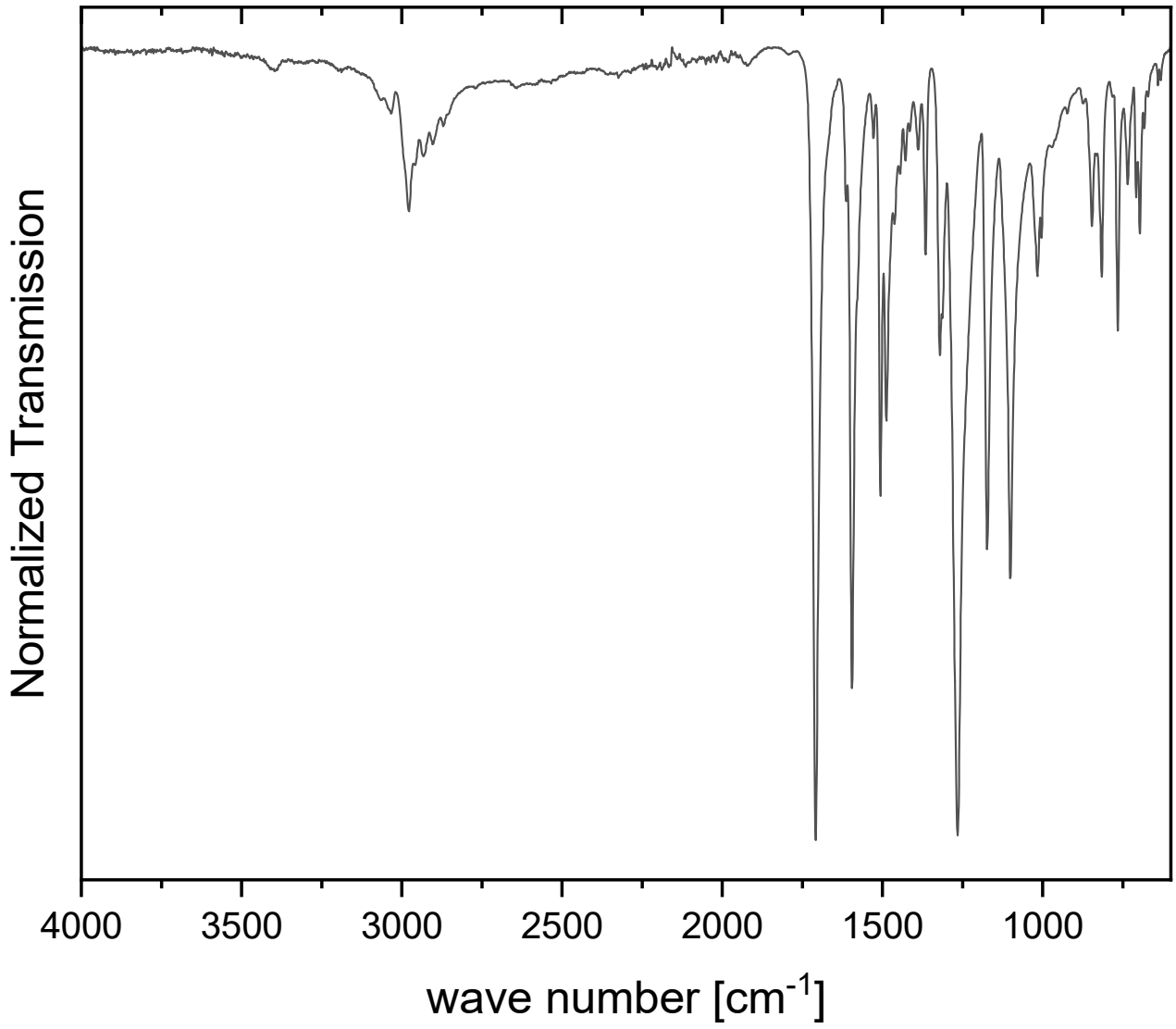

ESI Fig. S1: ATR-IR spectrum of Et_4tpdatb.

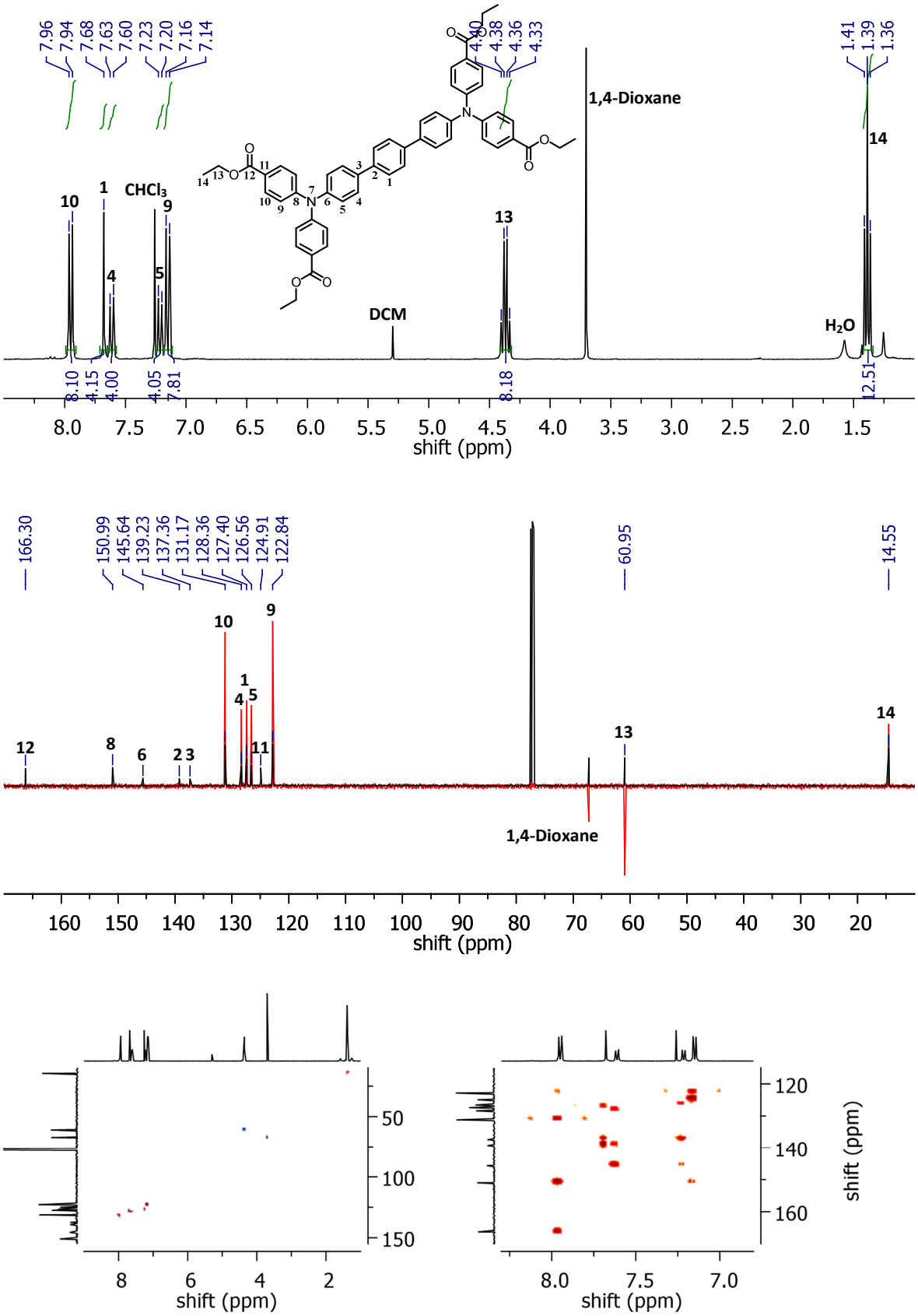

ESI Fig. S2: NMR spectra of Et_4tpdatb in DMSO-d_6. Top: section of the ^{1}H NMR (500 MHz), center: section of the ^{13}C NMR (126 MHz) (black) and dept-135 (red), bottom left: ^{1}H-^{13}C-HSQC, bottom right: section of the ^{1}H-^{13}C-HMBC.

1.2. H_4tpdatb

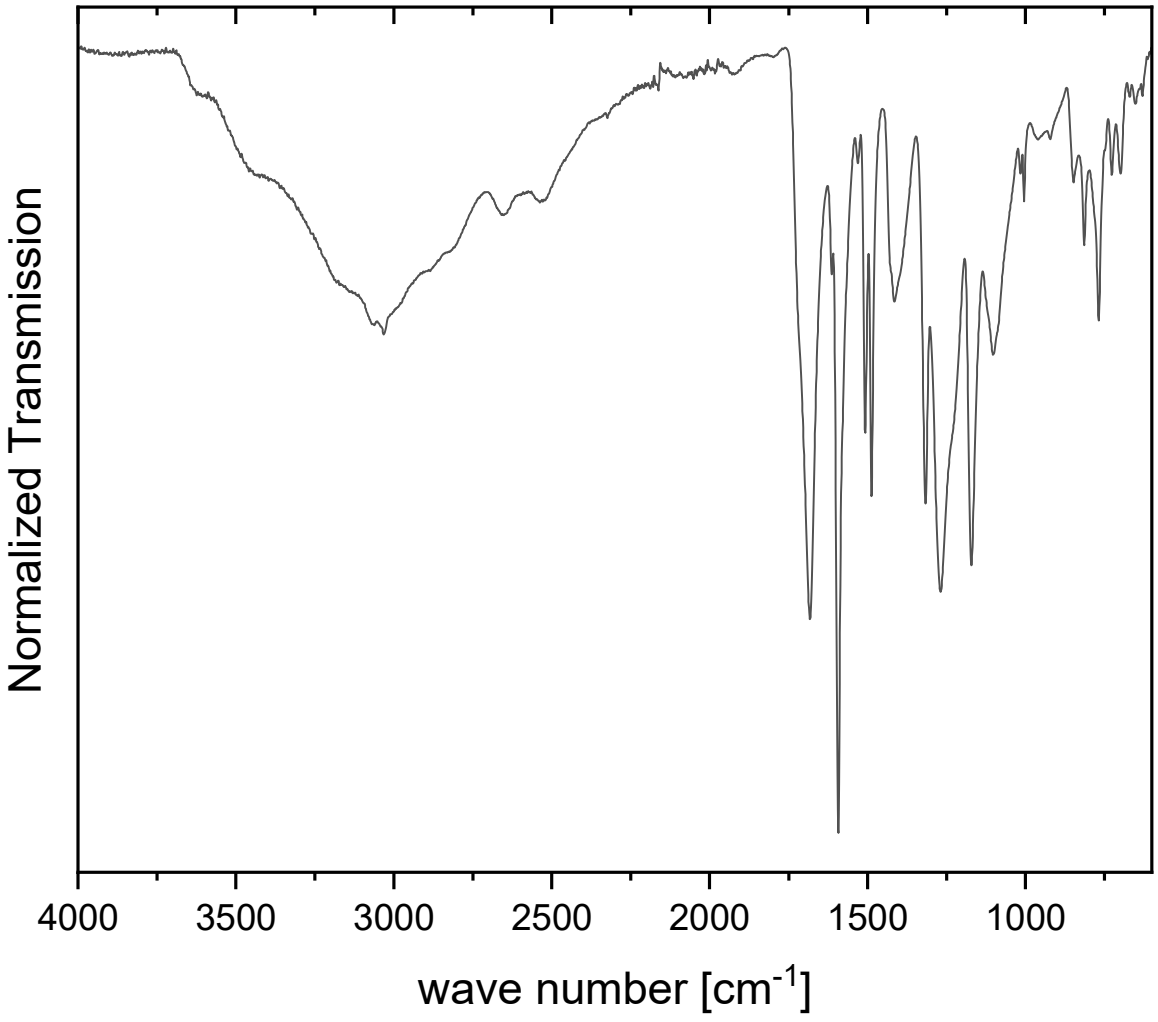

ESI Fig. S3: ATR-IR spectrum of the H_4tpdatb linker.

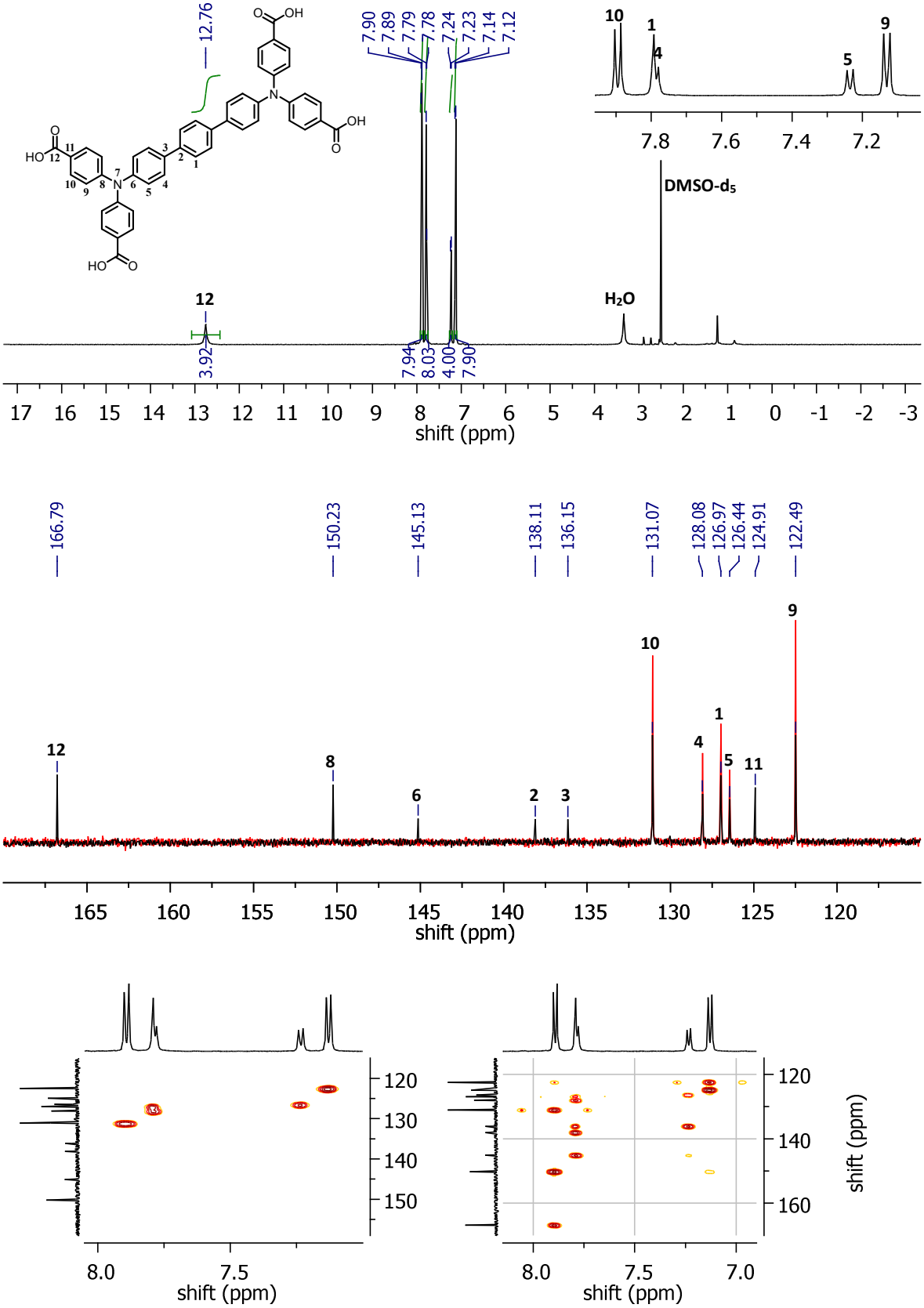

ESI Fig. S4: NMR spectra of H_4tpdatb in DMSO-d_6. Top: ^{1}H NMR (500 MHz), center: section of the ^{13}C NMR (126 MHz) (black) and dept-135 (red), bottom left: section of the ^{1}H-^{13}C-HSQC, bottom right: section of the ^{1}H-^{13}C-HMBC.

2. Additional Figures for MOF Characterization

2.1. DUT-180

ESI Table S1: Structure parameters of DUT-180op and DUT-180cp.

Unit cell parameter	**DUT-180op**	**DUT-180cp**
***a* (Å)**	23.363(14)	25.625(7) Å
***b* (Å)**	44.43(4) Å	46.937(6) Å
***c* (Å)**	17.167(10) Å	7.173(5) Å
α = β = γ	90 °	90 °
***V* (Å^3)**	17819.7 Å^3	8627.8 Å^3

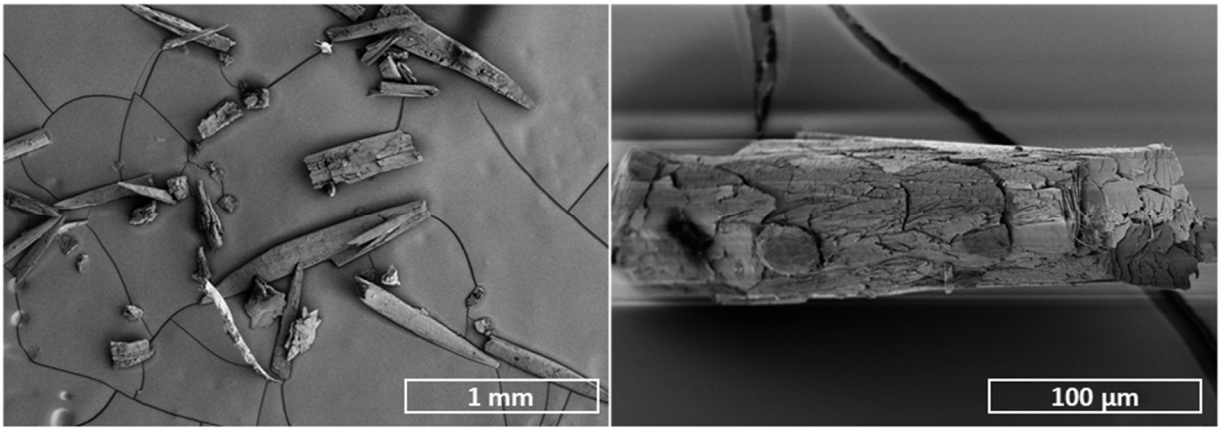

ESI Fig. S5: SEM images of activated DUT-180.

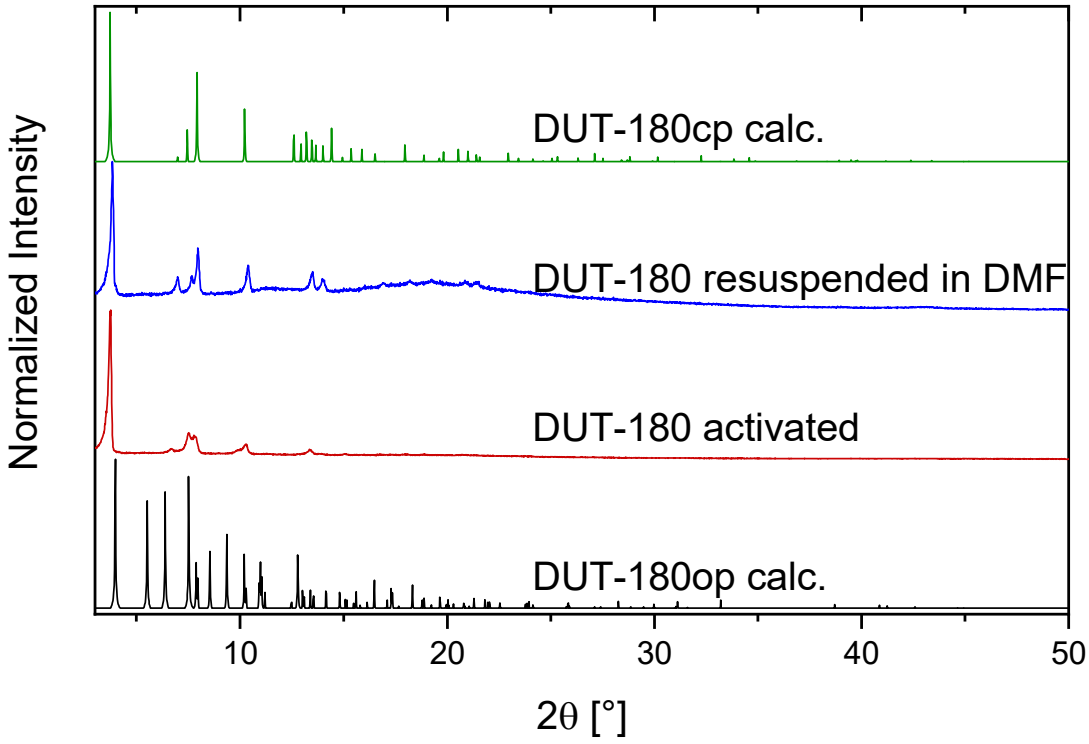

ESI Fig. S6: PXRD of DUT-180 activated and DUT-180 resuspended in DMF in comparison to theoretical PXRD patterns of DUT-180op and DUT-180cp.

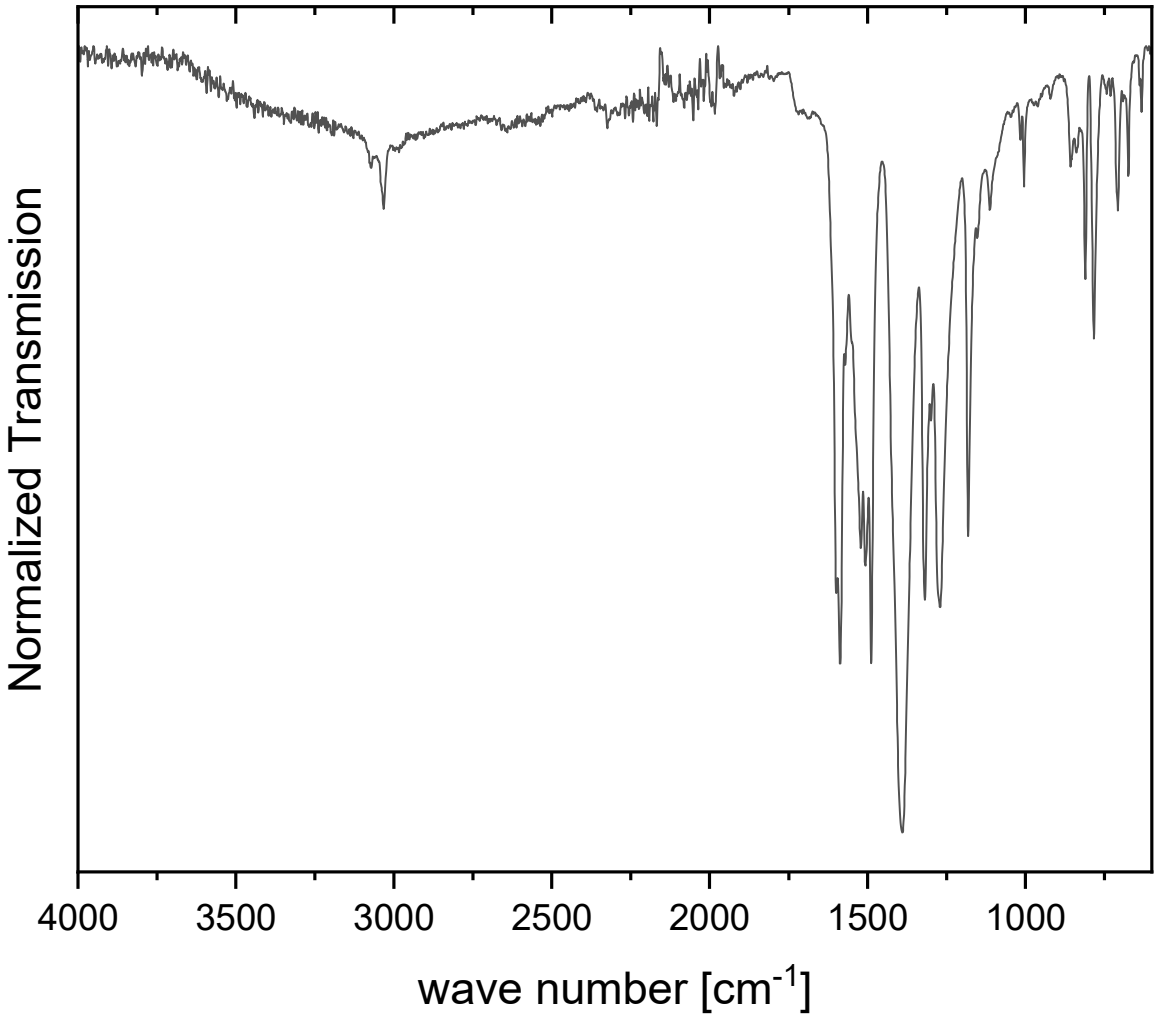

ESI Fig. S7: ATR-IR spectrum of activated DUT-180 stored under Argon atmosphere.

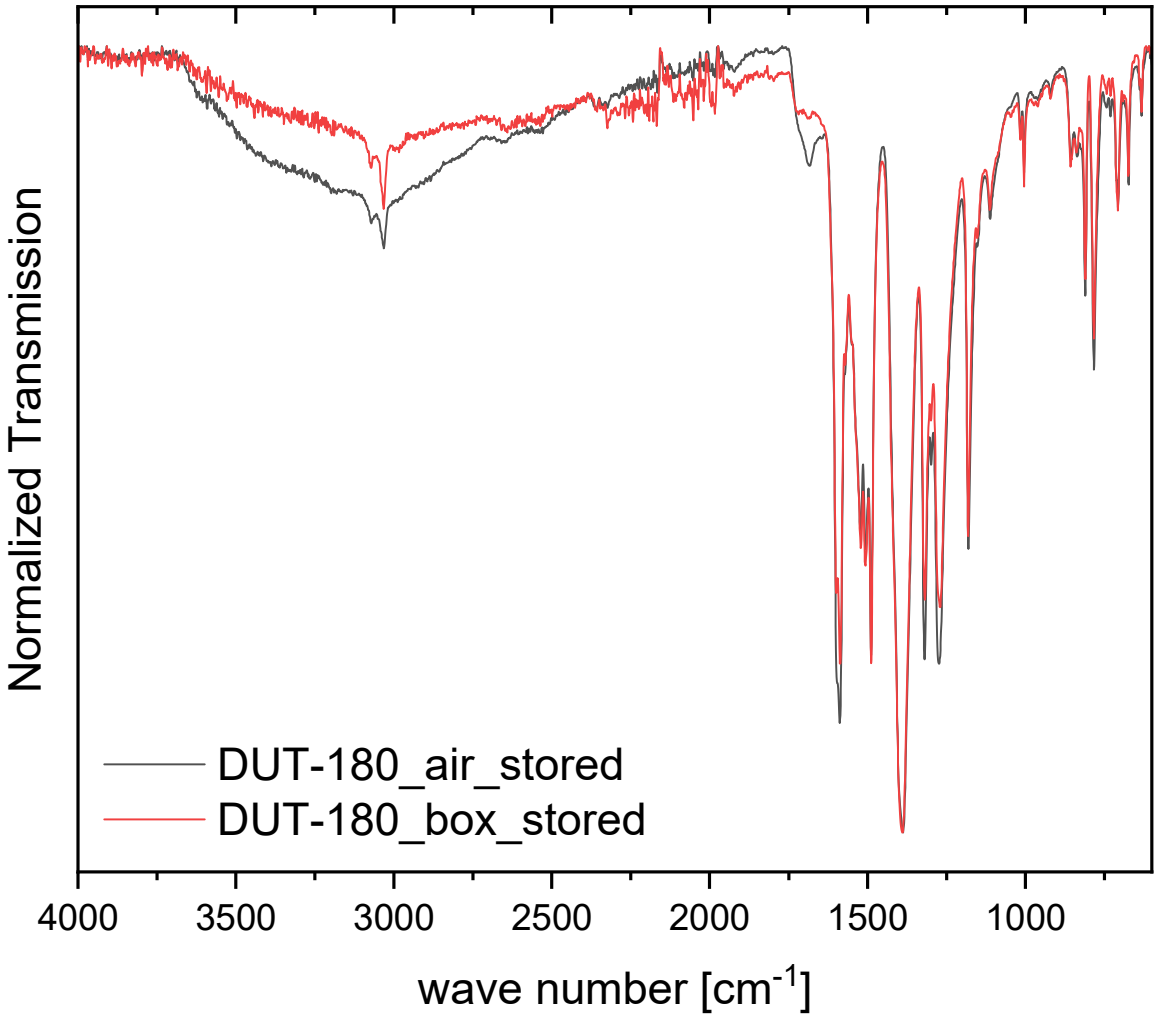

ESI Fig. S8: Comparison of ATR-IR spectra of activated DUT-180 stored under Argon in the glove box and DUT-180 stored under air for several weeks.

2.2. DUT-190

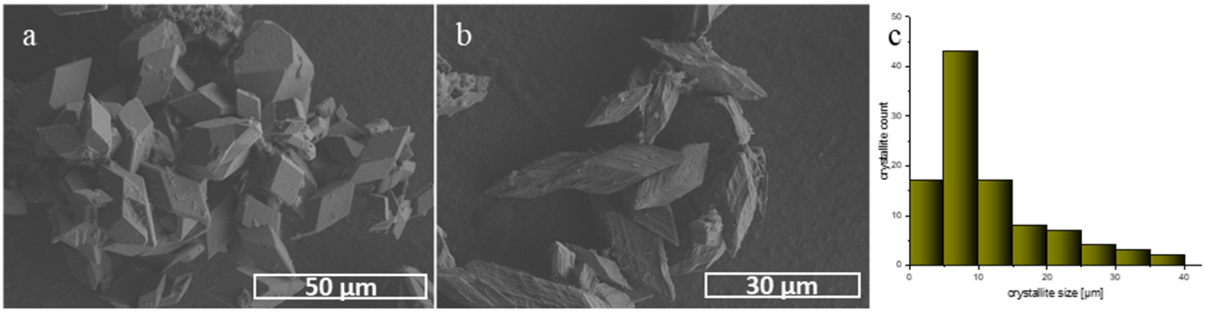

ESI Fig. S9: SEM before (a) and after (b) nitrogen physisorption as well as crystallize size distribution (c) before adsorption. The crystallize sizes refers to the edge lengths of the occurring crystals on several taken images.

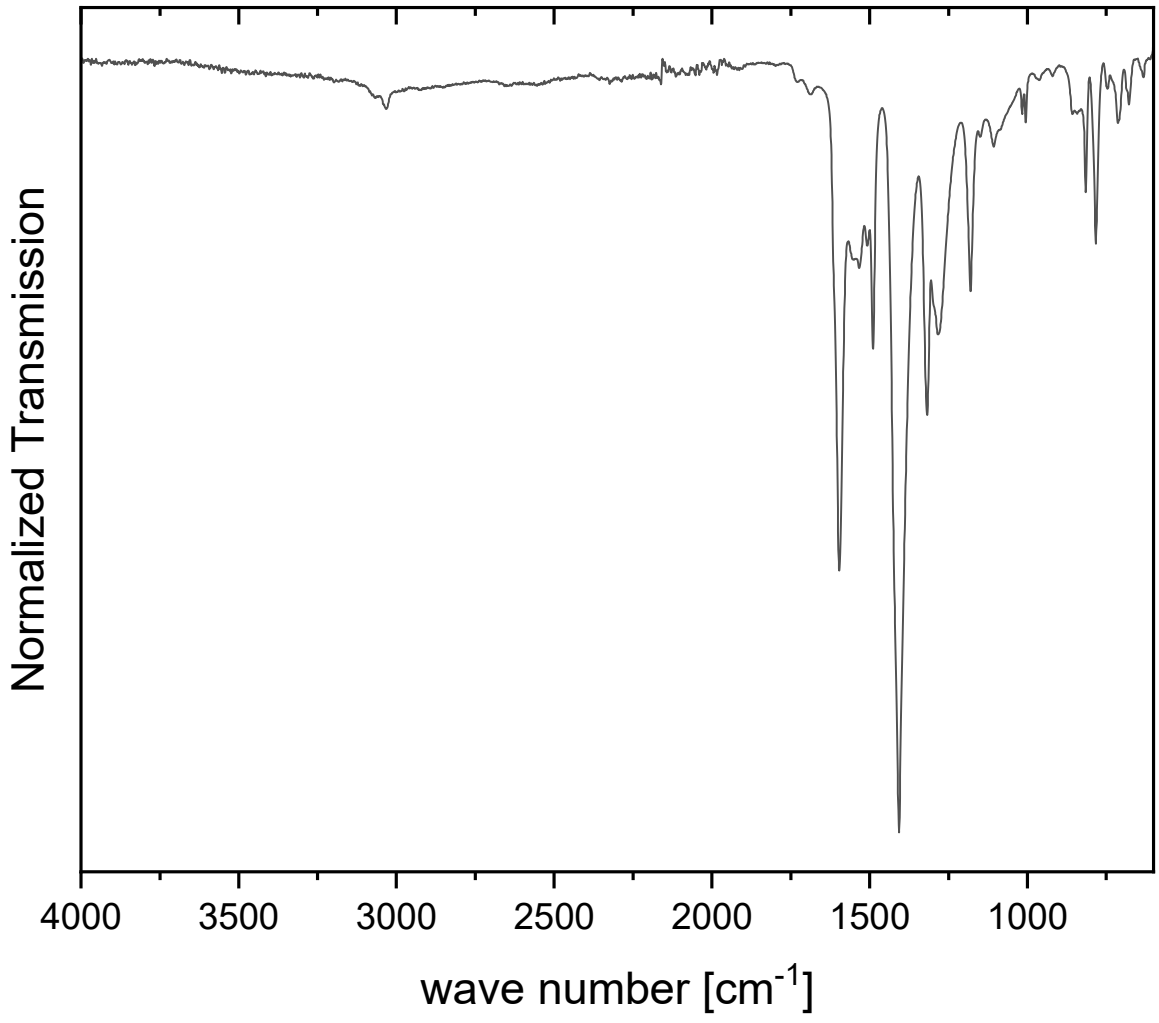

ESI Fig. S10: ATR-IR spectrum of activated DUT-190 stored under Argon atmosphere.

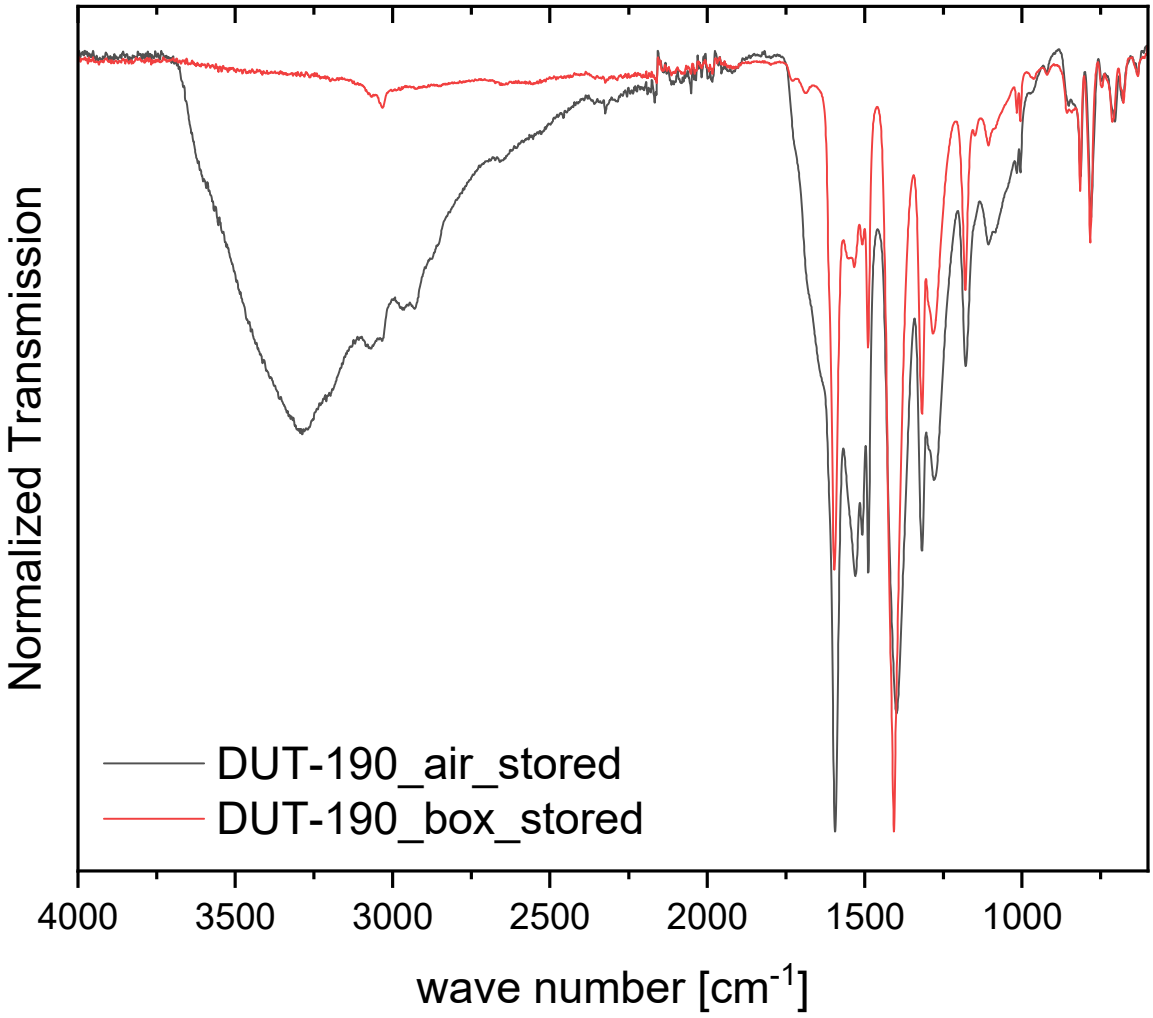

ESI Fig. S11: Comparison of ATR-IR spectra of activated DUT-190 stored under Argon in the glove box and DUT-190 stored under air for several weeks.

N_2 Physisorption

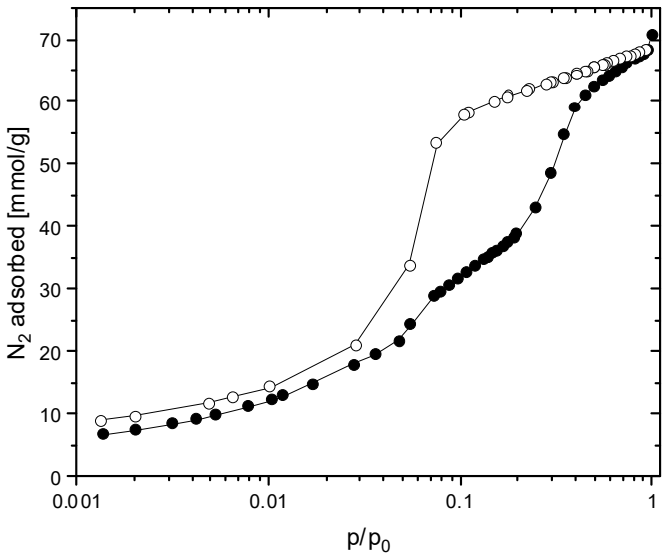

ESI Fig. S12: Semilogarithmic plot of Nitrogen physisorption isotherm at 77 K of the DUT-190 batch shown in **Fehler! Verweisquelle konnte nicht gefunden werden.**c, synthesized and activated by supercritical CO_2.

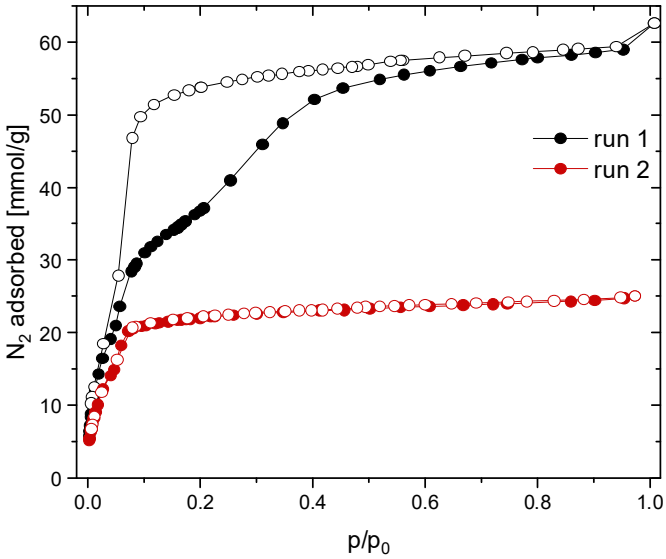

ESI Fig. S13: Isotherms of two runs of nitrogen physisorption at 77 K on DUT-190 without further activation between runs.

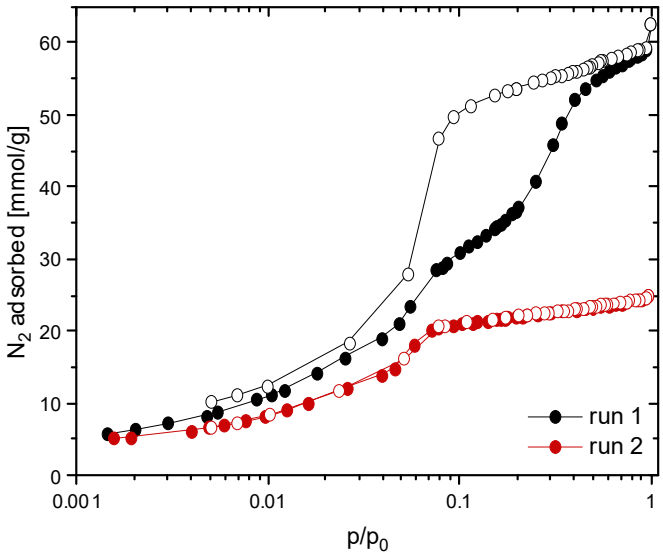

ESI Fig. S14: Semilogarithmic plot of Nitrogen physisorption isotherms at 77 K for the DUT-190 batch demonstrated in the previous figure.

CH_4 Physisorption

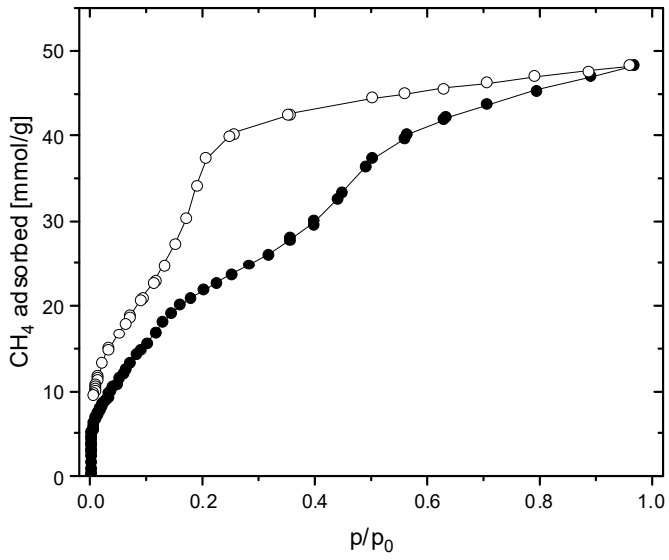

ESI Fig. S15: DUT-190 methane physisorption isotherm at 111 K, activated by supercritical CO_2.

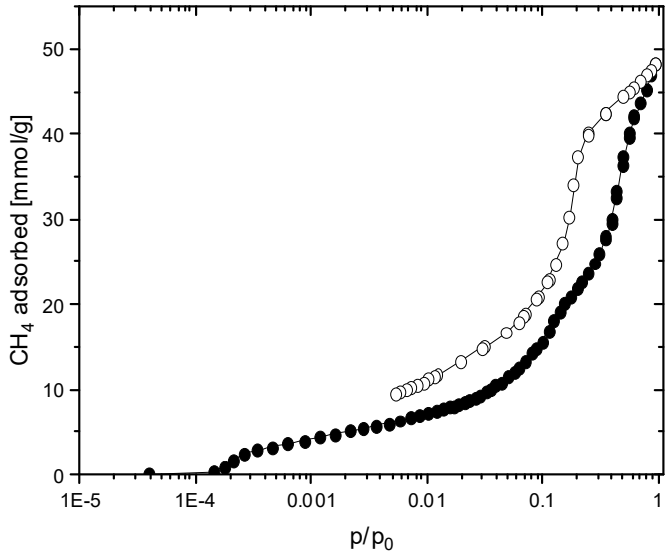

ESI Fig. S16: Semilogarithmic plot of DUT-190 methane physisorption isotherm at 111 K, activated by supercritical CO_2.

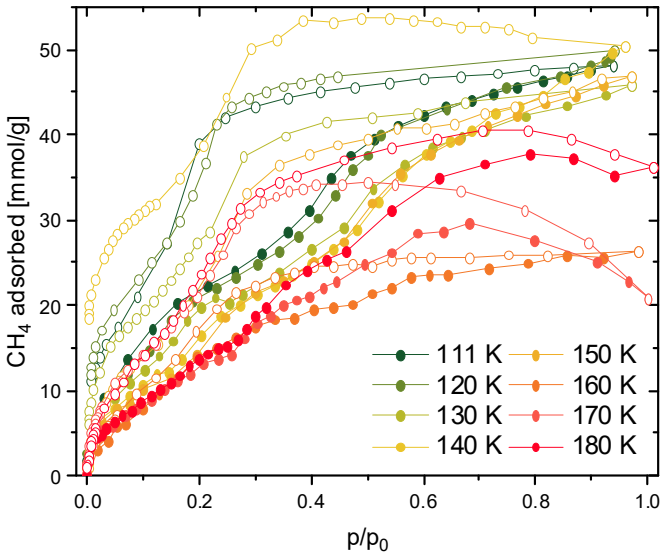

ESI Fig. S17: Methane Excess Adsorption of DUT-190 at various temperatures from 111 K up to 180 K using a new sample for each measurement.

CO_2 Physisorption

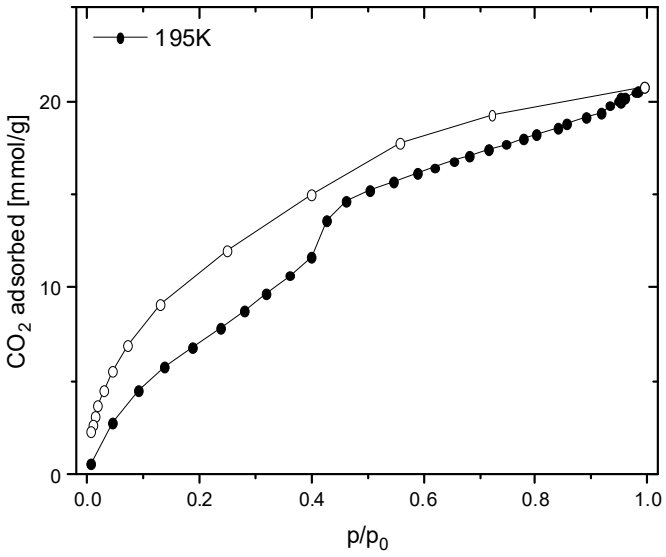

ESI Fig. S18: CO_2 Adsorption of DUT-190 at 195 K.

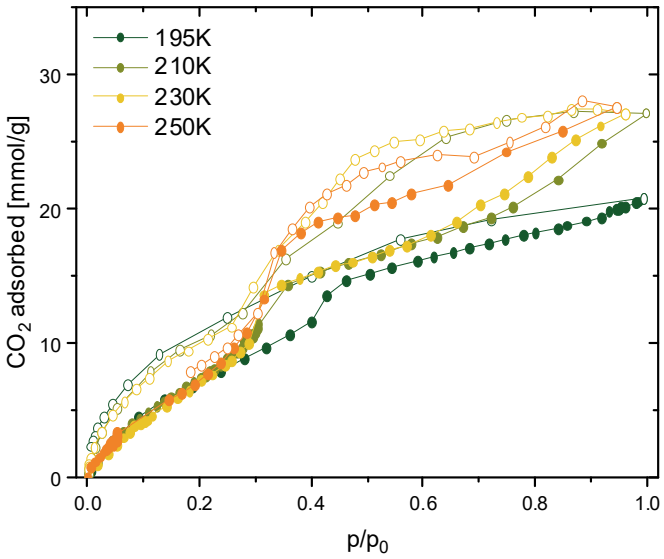

ESI Fig. S19: CO_2 Excess Adsorption of DUT-190 at various temperatures from 195 K up to 250 K using a new sample for each measurement.

Xe Physisorption

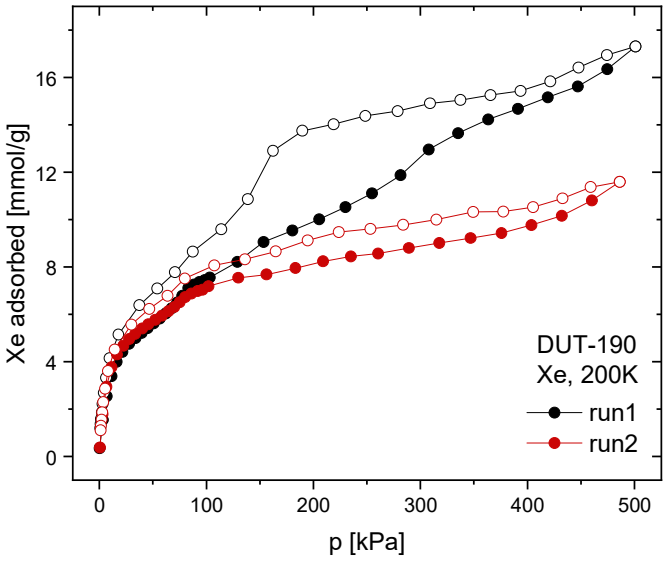

ESI Fig. S20: Two runs of Xe Excess Adsorption of DUT-190 at 200 K.

Crystal structures of contracted phases

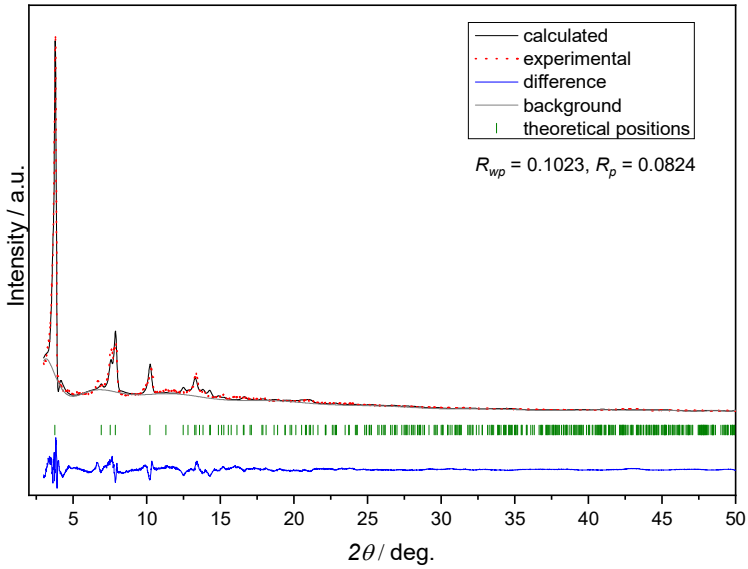

ESI Fig. S21: Rietveld plot for DUT-180cp.

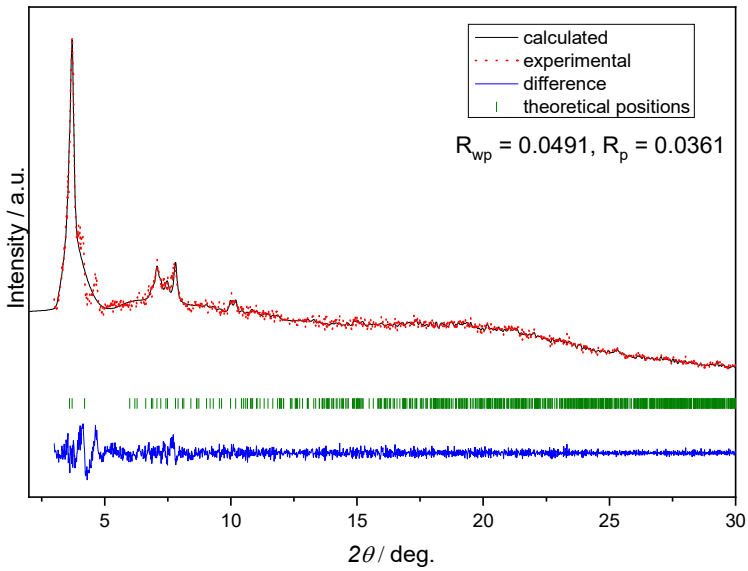

ESI Fig. S22: Pawley plot for DUT-190cp.

In situ PXRD in parallel to CO_2 physisorption at 195 K.

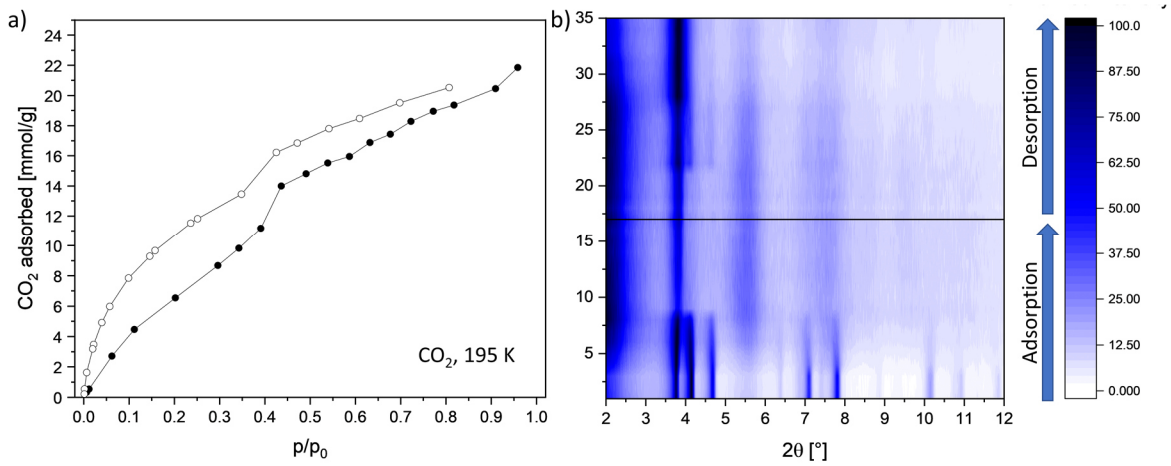

ESI Fig. S23: Physisorption isotherm of CO_2 at 195 K on DUT-190 (a) and PXRD patterns, measured in parallel to adsorption and desorption (b).

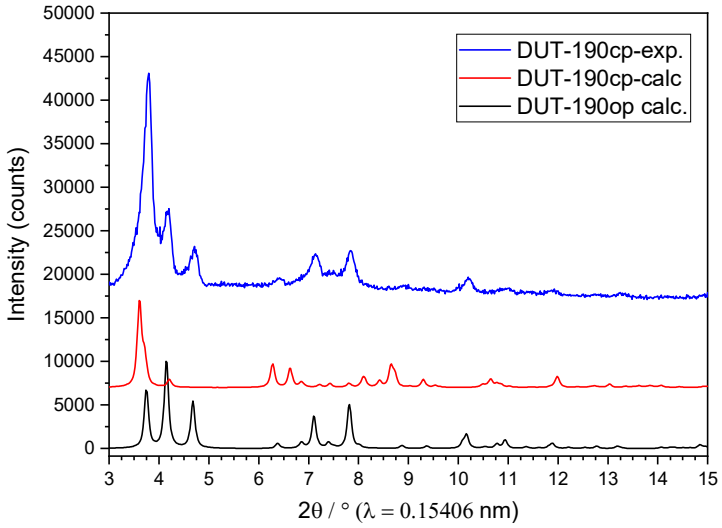

ESI Fig. S24: Calculated and experimental PXRD patterns of DUT-190op and DUT-190cp phases.

Geometrical pore size distribution

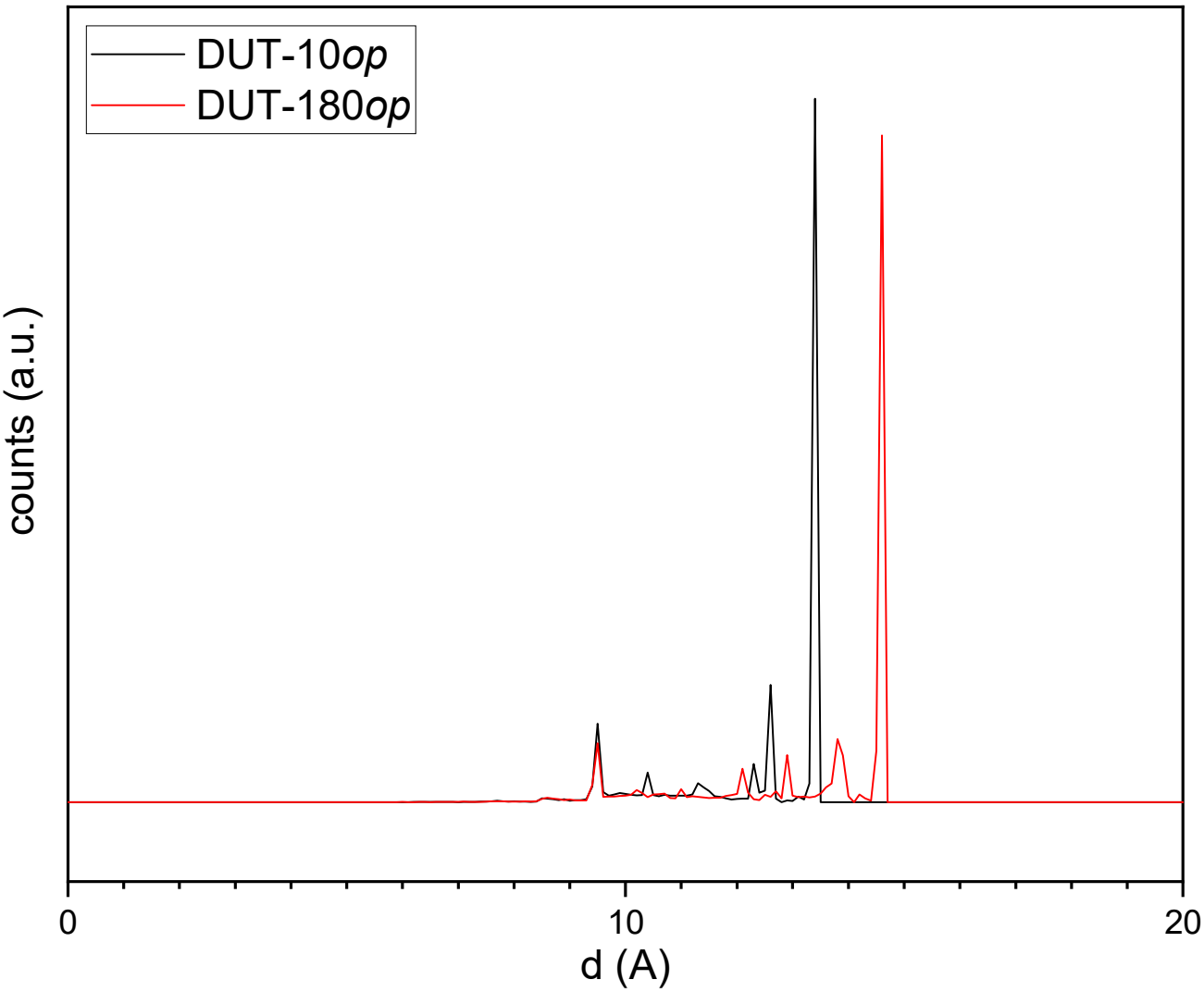

ESI Fig. S25: Pore size distribution of DUT-10*op* and DUT-180*op* in comparison.

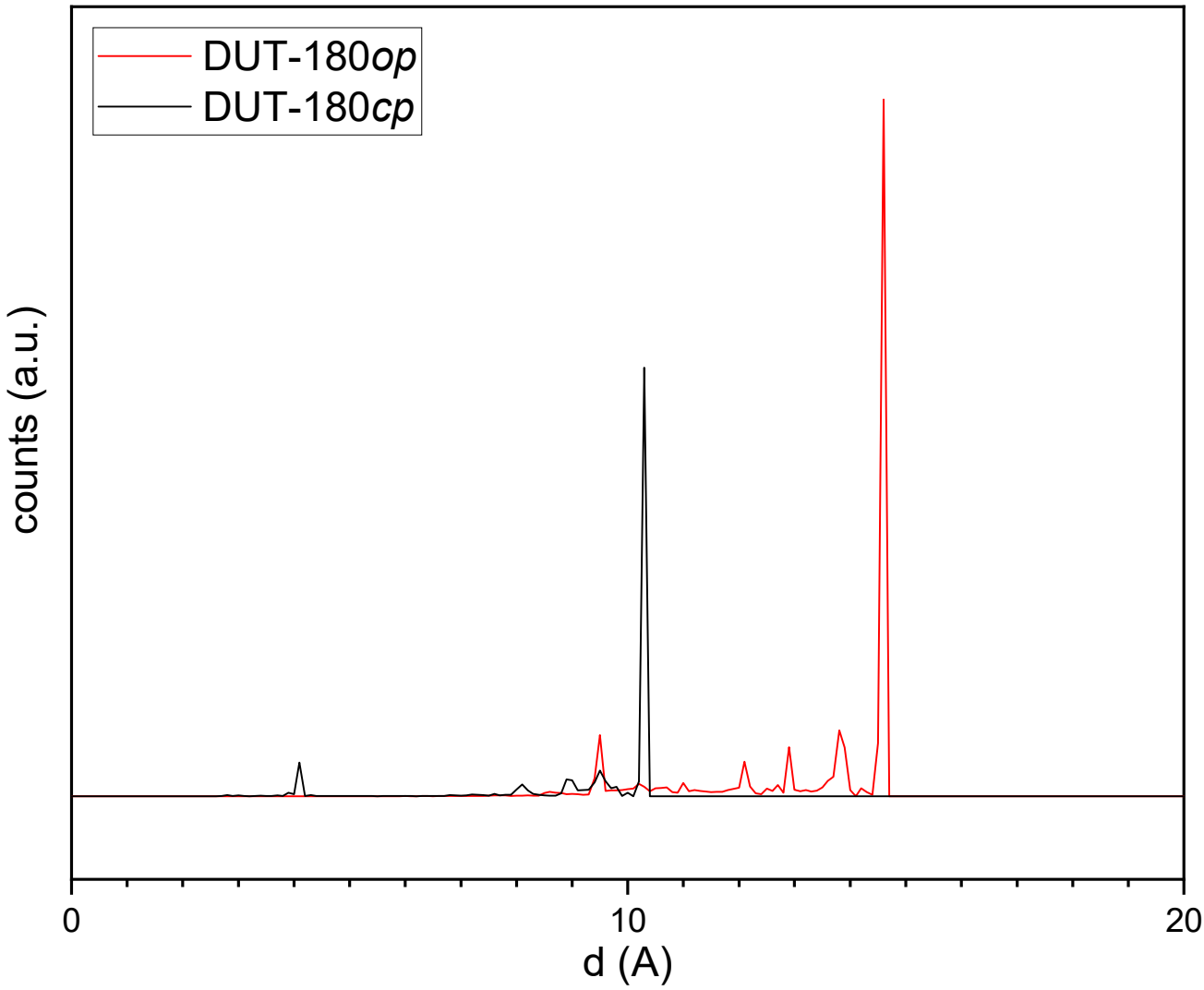

ESI Fig. S26: Pore size distribution of DUT-180*op* and DUT-180*cp* in comparison.

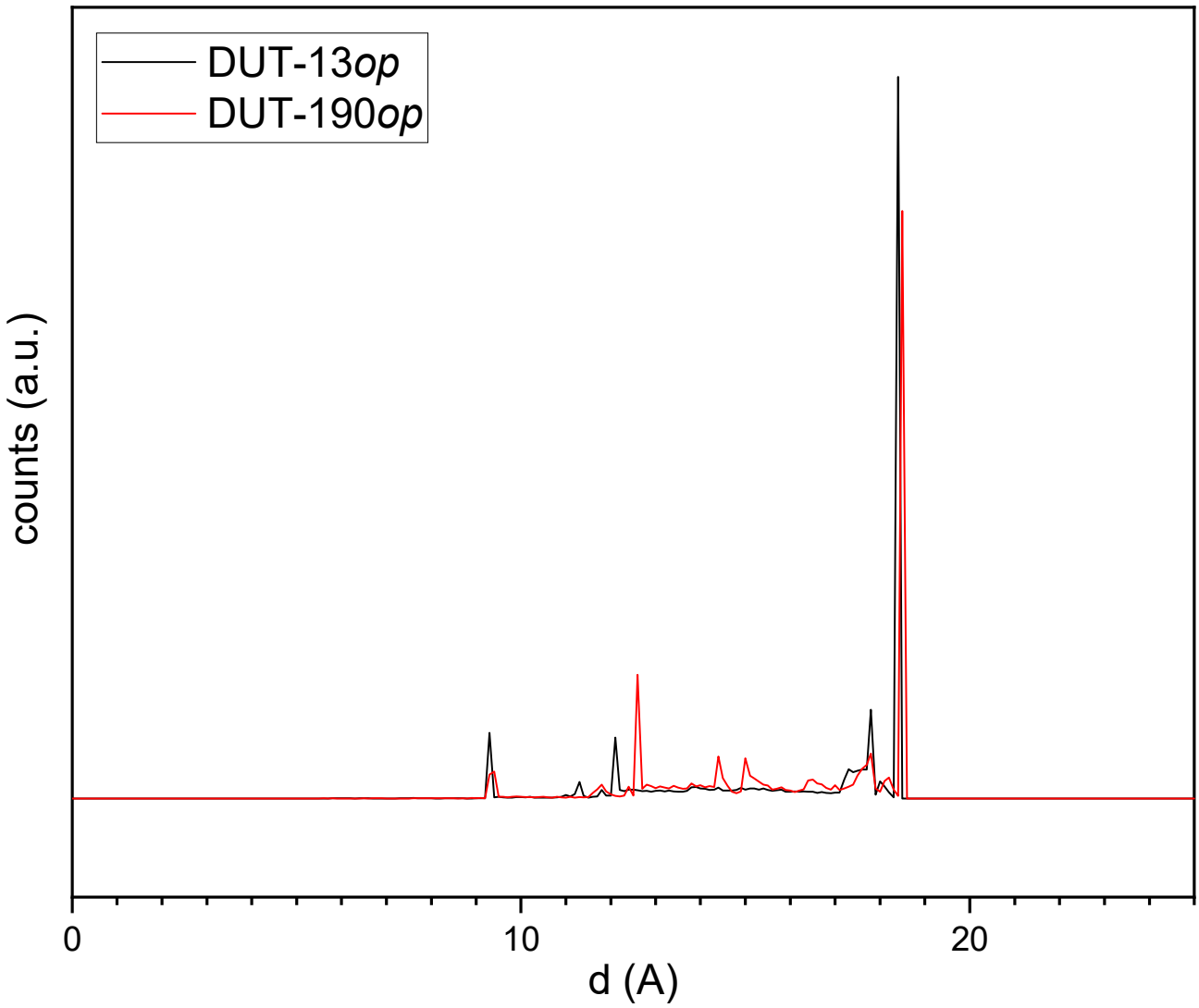

ESI Fig. S27: Pore size distribution of DUT-13*op* and DUT-190*op* in comparison.